Available online at www.tox.or.kr

Comparison of the Effects of Nano-silver Antibacterial Coatings and Silver Ions on Zebrafish Embryogenesis

Min-Kyeong Yeo[1] & Jae-Won Yoon[1]

[1]Department of Environmental Science and Engineering, KyungHee University, Yongin, Gyeonggi 449-701, Korea
Correspondence and requests for materials should be addressed to M. K. Yeo (bioclass@khu.ac.kr)

Accepted 12 January 2009

Abstract

To compare the effects of nanometer-sized silver ions and support materials (nano-silver coating material, NM-silver) and silver ions, we exposed zebrafish embryos to both types of nano-silver ions and compared the acute responses during embryogenesis. The amount of silver in the NM-silver (17.16%) was greater than that in the silver ion (4.56%). Both of these materials have different atomic compositions. The silver ion-exposed groups (10 and 20 ppt) showed lower survival rates than the NM-silver-exposed groups (10 and 20 ppt). NM-silver penetrated the skin and blood tube of zebrafish larvae as aggregated particles, whereas, silver ions penetrated the organelles, nucleus and yolk in a spread-out pattern. Microarray analysis of RNA from zebrafish larvae (72 hours post-fertilization) that were treated with either NM-silver or silver ions, showed alteration in expression of the BMP, activin, TGF-β, and GSK3β genes pathway. Additionally, GSK3β gene pathway for apoptosis that was related with left-right asymmetry. Gene expression changes in the NM-silver or silver ions-treated zebrafish embryo led to phenotypic changes in the hatched larvae, reflecting increased apoptosis and incomplete formation of an axis.

Keywords: Nano-silver antibacterial coatings, Silver ion, Biological toxicity, GSK3β, TGF-β, Zebrafish

Nanometer-sized silver materials are now used in various products, including fabrics, coating for baby bottles, cosmetic materials, toothpastes and washing machines[1,2]. The major property of nano-silver materials is their antibacterial effect[3,4]. Recent advances in nano-technology have increased the chances of contact between human and nano-sized materials including nano-sized silver. However, despite this increased exposure to nano-sized materials, little information is available regarding the toxicity of nano-sized materials in animals, including humans.

There are two types of nano-silver used in commercial products; one type is a coating that consists of nanometer-sized silver ions and support materials (nano-silver coating material, NM-silver)[5], and the other type is silver ions, which are produced by applying an electric current to a silver metal plate, such as in a washing machine or a drinking water machine[6]. In several studies, metal ions have been shown to have biological toxicity[7,8]. Moreover, these nano-silver ions have been shown to be biologically toxic; exposure to commercial nanometer-sized silver significantly affected Selenoprotein N gene expression in zebrafish embryos[5]. However, little is known about how nanometer-sized silver enters the cell. Furthermore, there are only a few comparative investigations of NM-silver and silver ions.

Accordingly, to compare the effects of NM-silver and silver ions, we exposed zebrafish embryos to both types of nano-silver ions and compared the acute responses during embryogenesis.

First, we analyzed the characteristics of both materials by SEM, TEM and energy dispersive X-ray (EDAX). Second, we investigated the biological effects of NM-silver (10 and 20 ppt) and silver ion (10 and 20 ppt) exposure during zebrafish embryogenesis by observing abnormal morphology and hatching rate. In addition, we used TEM to investigate whether NM-silver and silver ions can penetrate zebrafish cells. Finally, we used microarray analysis to investigate the genetic effects of NM-silver and silver ions on zebrafish larvae.

The Characterization of Commercial Nano-silver Coating Material and Silver Ions for Electrolysis

The size of the NM-silver and silver ion were about 20-30 nm (Figure 1). The atomic compositions on the nano-silver coating materials and silver ions are shown

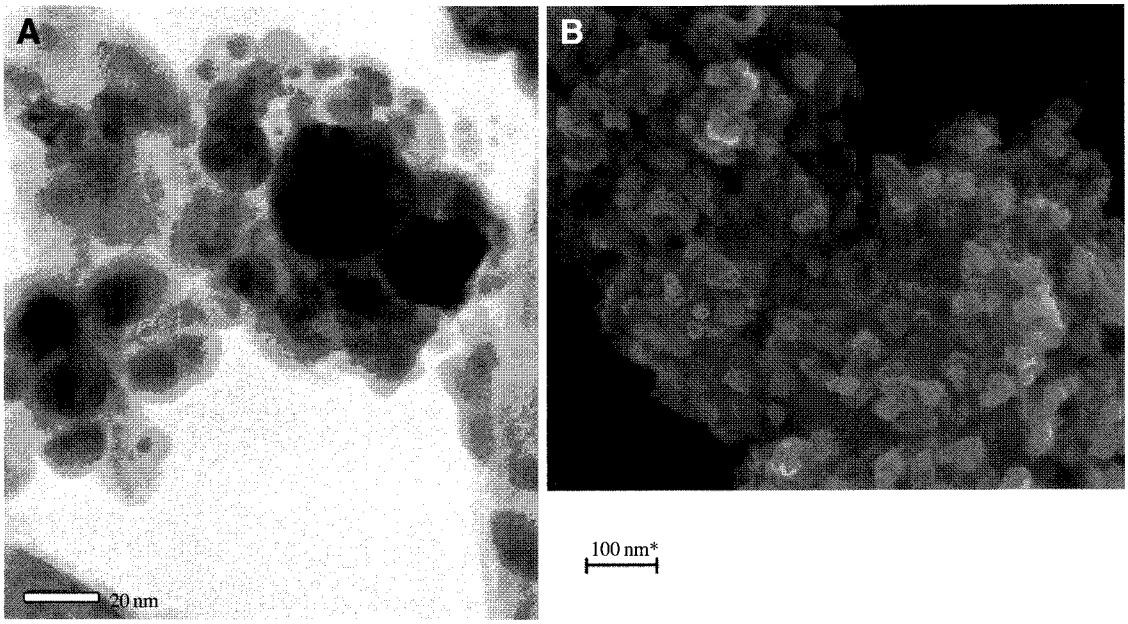

Figure 1. HRTEM analysis of nano-silver coating material (NM-silver) (A) and FE-SEM images of silver ions (B).

Table 1. The atomic composition of the nano-silver coating materials (NM-silver) and silver ions.

Materials	Composition on the surface (atomic %)							
	Ag		Ti		Cl		O	
NM-silver	17.16	:	0.06	:	0	:	41.69	
Silver ions	4.56	:	0	:	17.09	:	78.35	

in Table 1. The amount of silver in the NM-silver (17.16%) was greater than that in the silver ion (4.56%).

Both of these materials have different atomic compositions. Ti is used as a substrate to prevent the rejoining of the nano-silver. The NM-silver used as an antibacterial is an Ag-Ti composite. In a pre-study, we determined that the silver of NM-silver is of the ion form[5]. The silver ion that is produced by applying an electric current to a silver metal plate in the tap water has Cl, resulting in AgCl produced in a silver ion solution.

The Phenotypes of Zebrafish Larvae Exposed to The Nano-silver Coating Material or Silver Ions

In zebrafish larvae exposed to NM-silver or silver ions at 72 h post-fertilization (hpf), similar morphological defects of the heart were observed, such as a thin and string-like shape, pericardial edema and blood pooling (Figure 2C, D, E). These defects initially occurred in 2-day postfertilization (dpf) morphants, and then were predominantly observed in 72-hpf morphants. Although the heart defects were similar between zebrafish embryos exposed to NM-silver and those exposed to silver ions, the defects of the silver ions morphants were more severe than those of the NM-silver morphants (Figure 2B, C vs. Figure 2D, E). Around 30% of the silver ion morphant defects were lethal due to an absent body axis at 72 hours (Figure 2E). In addition, apoptosis was observed in the heads of several larvae (Figure 2F) and the remainder of the surviving morphants exposed to the NM-silver suffered from incomplete formation of an axis (Figure 2C), suggesting that nanometer-sized silver and silver ions may function differently during cardiogenesis, even though they cause similar heart defects. We also noticed that the specific abnormal morphologies/total of surviving individuals (%) was dependent on the concentration of the NM-silver and silver ions (Figure 3). When 10 ppt of NM-silver was used to treat the zebrafish during embryogenesis, we found that 16.48% of embryos displayed a defected heart; whereas when 20 ppt NM-silver was used, 13% of embryos appeared to have a similar heart defect. Further, 20 ppt silver ion caused 37% of embryos to suffer heart damage at 72 hpf, whereas 10 ppt silver ion caused 33% of embryos to have similar heart damage. These results indicate that the effects of NM-silver and silver ion on embryogenesis are dosage-dependent and specific.

Furthermore, edema and an abnormal notochord were observed in both exposure groups (NM-silver and silver ion). The survival was measured by the hatching rate (%). The silver ion-exposed groups (10

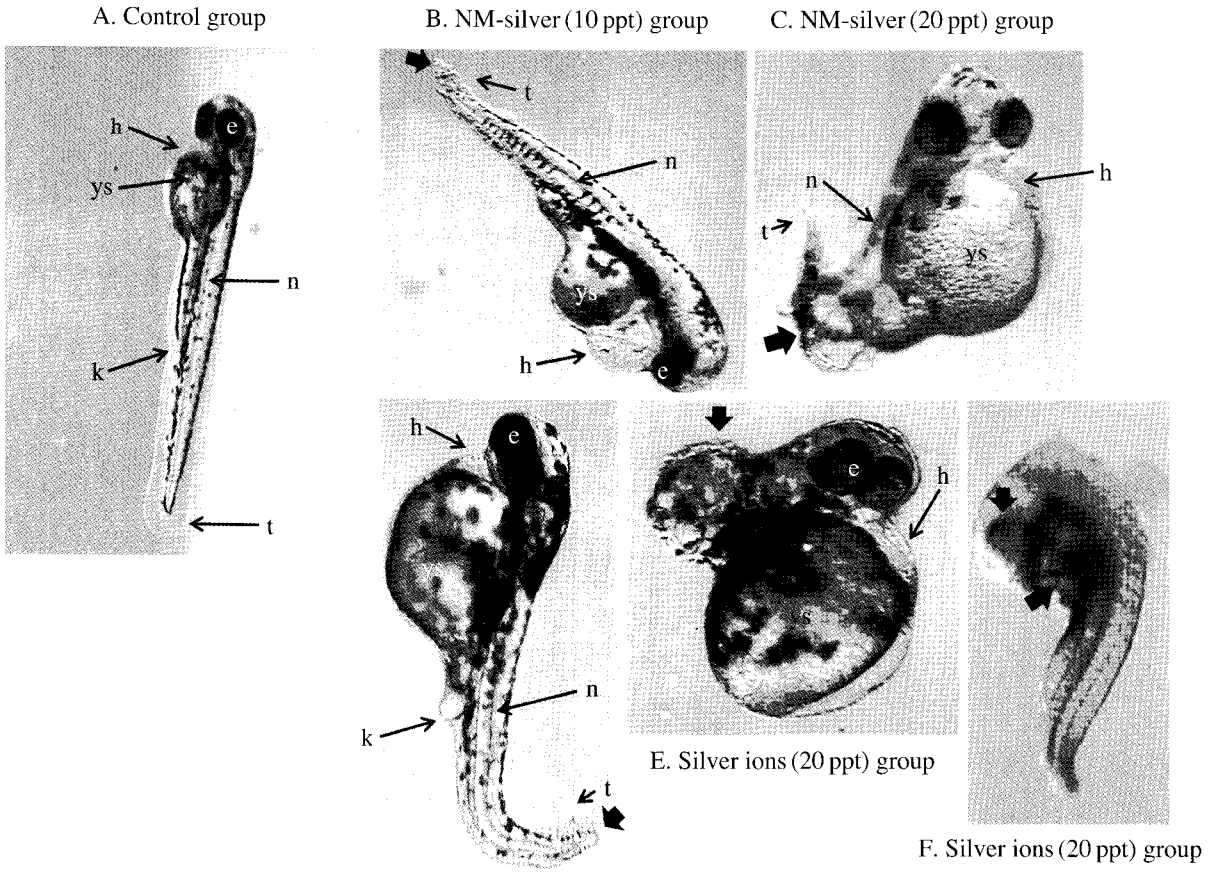

Figure 2. Comparison of the effects of nano-silver coating materials (NM-silver) and silver ions on the development of zebrafish. Embryos were exposed to NM-silver at 10 and 20 ppt (B, C) and silver ions at 10 and 20 ppt (D, E, F). These images show zebrafish exposed to each treatment at 72 hpf. The thick arrow indicates the apoptosis point. Abbreviations: h, heart; e, eye; n, notochord; t, tail; ys, yolk sac; k, kidney.

and 20 ppt) showed lower survival rates than the NM-silver-exposed groups (10 and 20 ppt).

Histological Analysis of The Effects of Nano-silver Coating Material and Silver Ions in Zebrafish Cells

Our results show that NM-silver and silver ions can penetrate zebrafish cells (Figure 4). Moreover, NM-silver penetrated the skin (Figure 4A) and blood tube (Figure 4B) of zebrafish larvae as aggregated particles, whereas, silver ions penetrated the organelles, nucleus (Figure 4C) and yolk (Figure 4D) in a spread-out pattern. However, the range of penetration in the cell was similar between the NM-silver and silver ion.

Changes in Gene Expression Profile

We compared the gene expression profiles of zebrafish embryos treated with either NM-silver or silver ions (Table 2). The transforming growth factor-β (TGF-beta) signaling superfamily members, pitx2a, acvr2b and smad1, were up regulated 1.3- to 2.3-fold, while one family member, InhbB, was significantly down regulated. The genes, mapk8 and GSK3β, were down regulated in the silver ion-exposed groups compared to in the NM-silver-exposed groups. Based on the expression profile changes that occurred after treatment with nano-materials (NM-silver or silver ions), a model pathway for apoptosis that was related with left-right asymmetry in zebrafish (Figure 5).

Discussion

The EDAX analysis confirmed that commercial NM-silver and silver ions are composed of silver (Table 1). Because the silver of NM-silver is unstable in the

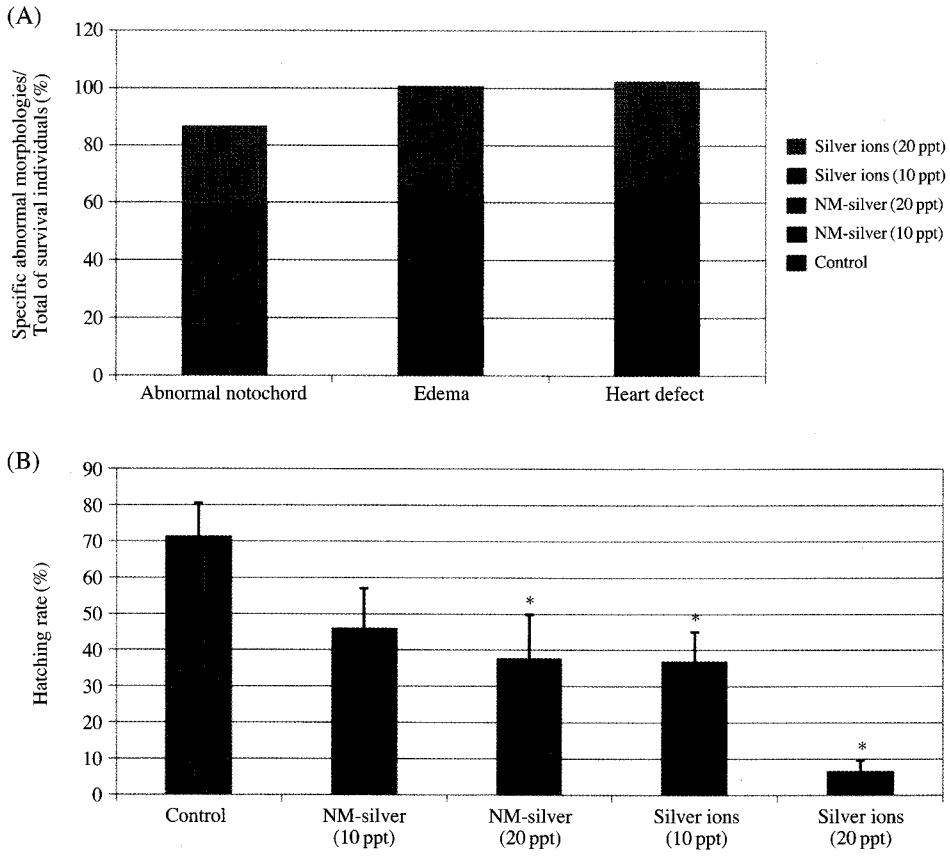

Figure 3. Rates of specific abnormal morphologies among surviving embryos are shown (A). The abnormal morphologies included abnormal notochord, edema and heart defect. The effects of NM-silver and silver ions on the hatching rate (B). The hatching rate decreased in groups exposed to NM-silver and silver ions (10 ppt and 20 ppt) compared to the control group.

ion form, Ti substrate is used to help maintain the nanometer-sized ion form. Silver ions that are produced by applying an electric current to a silver metal plate, such as in a washing machine, include Cl, with a percentage ratio of silver to Cl of 4.56 : 17.09. Based on this, we suggest that the silver ion attaches to Cl to produce AgCl. The sizes of both silver ions and NM-silver are around 20-30 nm (Figure 1A and B). The ionic form potentially increases the antibacterial effect[9] and the nanometer size results in an increased surface area. These results suggest that NM-silver should be used in the ionic form for antibacterial applications. If the nanometer-sized materials rejoin to form a complex, however, their properties are likely to change. In this study, the NM-silver coating material was Ag-Ti composites, as antibacterial coatings contain more than one substance, but other commercial nano material composites can be manufactured with multiple types of surface ligands. We suggest that these manufactured nano materials create new challenges for ecotoxicity testing. Moreover, silver ions of NM-silver and silver ion solution by electrolysis that bonds to other materials may result in a secondary contaminant that can impact the ecosystem. In addition, the properties of the nanometer-sized silver ions are likely to be lost upon binding to another material. Nanometer-sized silver ions that are not bound to another molecule can penetrate cells. Permeation and accumulation of silver ions with NM-silver and silver ion solution were shown in the membrane, nuclei and blood vessels of zebrafish cells (Figure 4). The relationship between size and migration into cells observed in this study corresponds to that reported by several other researchers[10-13].

The penetration of these nano-sized silver ions has the effect of metal ions on a living organism. Ag ions are a type of metal ion, and metal ions, such as Mg^{2+}, act as cofactors for enzymes that cleave or synthesize DNA[14,15], using nucleotides as substrates[15,16]. In addition, Ag^{+} is known to undergo strong covalent binding with DNA[16].

The phenotypes of zebrafish embryos exposed to either NM-silver or silver ions are shown in Figure 2. Similar morphological defects of the heart were observed after NM-silver and silver ion exposure in zebrafish larvae at 72 hpf, including a thin shape and pericardial edema (Figure 2B, C, D, E). In the silver ion-exposed group, around 30% of the morphant defects were lethal due to an absent body axis at 72 hours (Figure 2E), suggesting that nanometer-sized silver

NM-silver

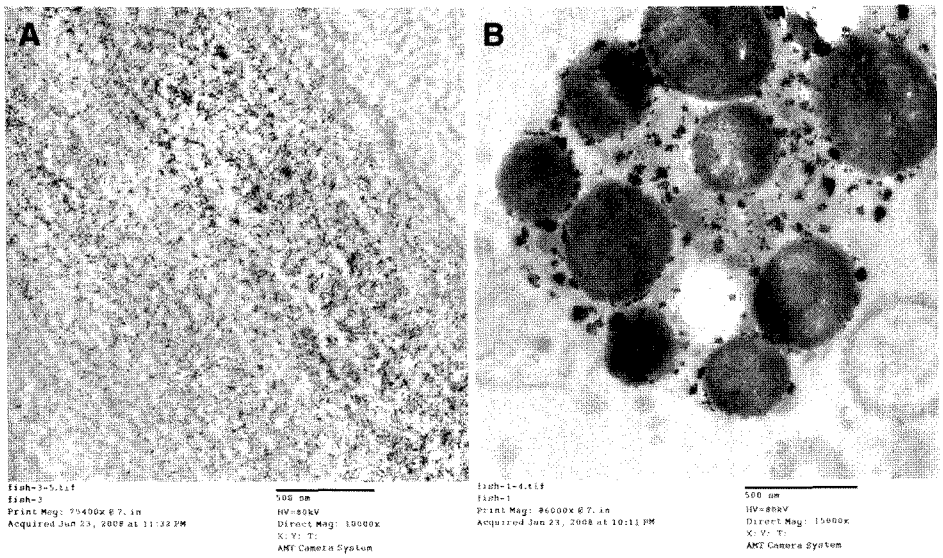

Scale bar 500 nm, Direct Mag: 10000X

Scale bar 500 nm, Direct Mag: 15000X

Silver ions

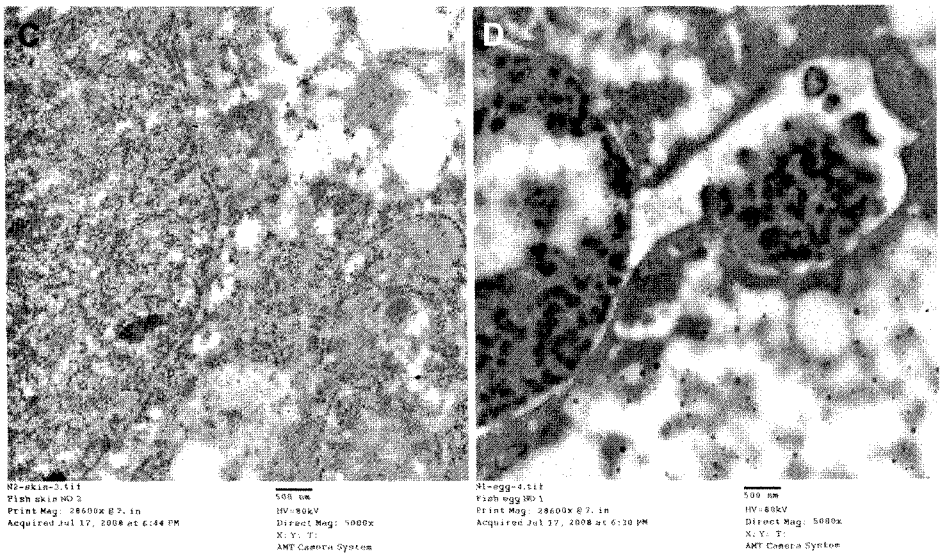

Scale bar 500 nm, Direct Mag: 5000X

Scale bar 500 nm, Direct Mag: 5000X

Figure 4. TEM images of zebrafish larvae (A : epidermis, B : blood vessel, C : nucleus) and zebrafish embryogenesis (D) after exposure to NM-silver and silver ions. Both of the nanometer materials penetrated the cell.

and silver ions may function differently during cardiogenesis, even though they cause similar heart defects. These abnormal phenotypes associated with GSK3β expression involve the modulation of left-right asymmetry and heart positioning[17]. In our microarray analysis, glycogen synthase kinase 3 beta (GSK3β) expression showed a greater down regulation in the silver ion-exposed groups than in the NM-silver groups (Table 2 and Figure 5). Moreover, we observed a reduced number of cardiomyocytes in the GSK3α morphants during the heart-ring stage, which was due to apoptosis[17]. GSK3α (51 kDa) and GSK3β (47 kDa) are two closely related GSK3 isoforms encoded by distinct genes[18]. The difference in size is due to a glycine-rich extension at the N-terminus of GSK3α. GSK3α and GSK3β are highly homologous within their kinase domains[19].

In this present study, several larvae showed apoptosis occurring in the head (Figure 2F), which is a phenotype previously reported in the heads of GSK3α

Table 2. Gene expression of zebrafish transcripts in response to exposure to nano-silver coating material (NM-silver) or silver ions, according to gene ontology.

Gene symbol	Gene description	NM-silver	Silver ions	Categories
pitx2a	paired-like homeodomain transcription factor 2a	1.3071525	2.081685	Multicellular organismal development, regulation of transcription
acvr2b	activin receptor IIb	1.8797202	2.2645829	cartilage development, hindbrain development neural crest cell migration protein amino acid phosphorylation, skeletal development transmembrane receptor protein serine/ threonine kinase signaling pathway
inhbb	inhibin, beta B	0.41046774	0.38466948	oocyte differentiation, growth factor activity, hormone activity
smad1	MAD homolog 1	1.9541554	2.3198686	BMP signaling pathway, embryonic pattern specification, regulation of transcription
smad2	MAD homolog 2	0.80638605	0.69233346	embryonic pattern specification, intracellular signaling cascade, regulation of transcription, DNA-dependent
mapk8	mitogen-activated protein kinase 8	0.7998309	0.40123546	protein amino acid phosphorylation, MAP kinase activity
GSK3β	glycogen synthase kinase 3 beta	0.788188	0.390299	ATP binding, kinase activity, nucleotide binding, protein kinase activity, protein serine/threonine kinase activity, transferase activity

knockdown embryos[17]. Moreover, the remainder of the surviving morphants from the nano-silver coating material-exposed group and silver ion-exposed group suffered from incomplete formation of an axis (Figure 2C, E), which is related to the pronounced apoptosis observed throughout the axis[17,20].

The transforming growth factor ligand activin plays important roles in mesendoderm induction and patterning during vertebrate embryogenesis. Activin is believed to transduce a signal through the receptor-activated transcription factor smad2. Knockdown of smad2 fails to block mesodermal development[21].

In this study, members of the transforming growth factor-β (TGF-β) superfamily (pitx2a, acvr2b and smad1) were more up regulated in the silver ion-exposed groups than in the NM-silver-exposed group, with the exception of the inhbb gene, which was down regulated (Table 2). The TGF-β superfamily is thought to regulate the specification of a variety of tissue types in early embryogenesis. The zebrafish activin type II receptor, ActRIIb, has dual roles in both activin and BMP (bone morphogenetic protein) signaling pathways during zebrafish embryogenesis[22]. The phenotype presented in Figure 2(C, E) represents an uncoordinated embryo at high doses of ActRIIb mRNA injection[22]. Overexpression of ActRIIb in zebrafish embryos causes dorsalization of embryos, which was observed more frequently in activin-overexpressing embryos that were exposed to silver ions than in those exposed to NM-silver (Table 2).

It has been suggested that these nano-silver ions induce signals from ActRIIb through the specific type I receptors, TARAM-A and BMPRIA, for activin and bone morphogenetic protein (BMP), respectively.

Materials and Methods

The Characterization of Commercial Nano-silver Coating Material and Silver Ions by Electrolysis

The commercial NM-silver was purchased from N corporation (Korea) and diluted with water to a concentration of 500 ppm. This type of silver is widely used within nano-silver products in Korea, including baby bottles, socks and underwear. The silver ions were produced via the electrolysis of pure Ag electrodes in 1 L of the tap water with an electronic voltage

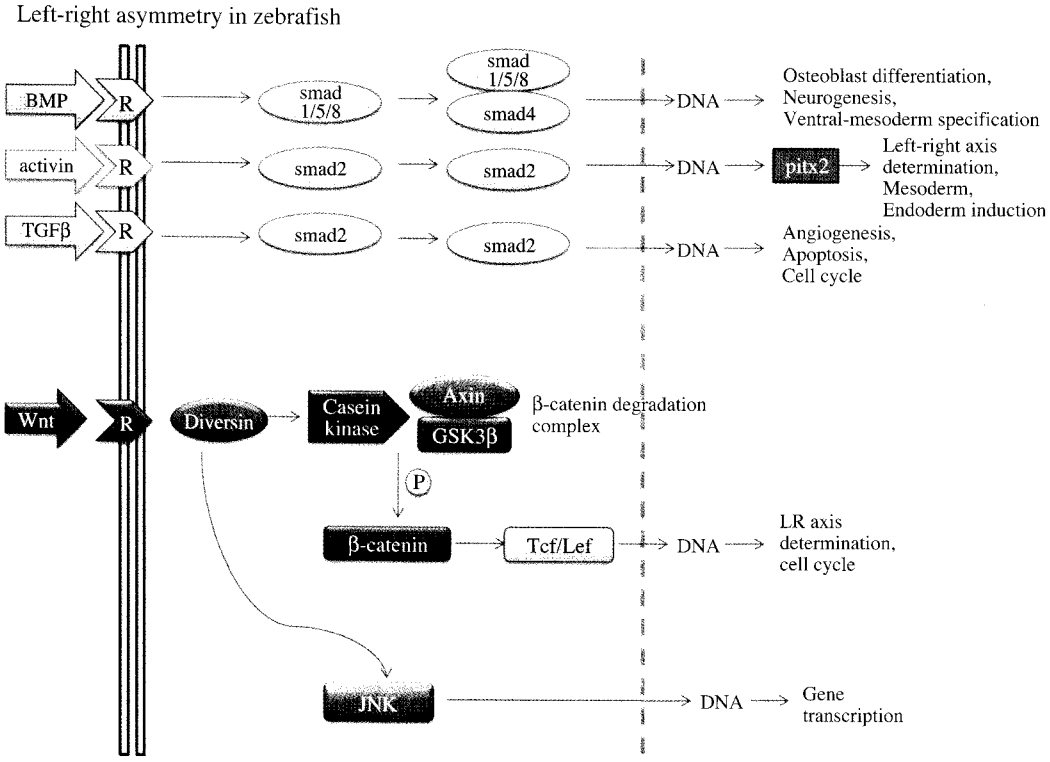

Figure 5. Model pathway of genes related to apoptosis and left-right asymmetry in zebrafish.

of 100 V[23]. The concentration of the silver ion solution was approximately 2.22 ppm, which was determined by ICP at the Kyung Hee University. The size, shape and composition of the nano-silver particles and ions were observed by scanning electron microscopy (SEM, model JEOL-JSM35CF). The power and working distance were set to 15 kV and 39 cm, respectively. In addition, a HRTEM (High Resolution Transmission electron Microscope, JEOL, Japan), with an accelerating voltage of 300 kV, was used to study the structure and morphology of the nano-silver[13]. An energy-dispersive X-ray spectrometer (EDX) was used to determine the chemical composition on the nano-silver particles and ions.

Experimental Animals

The zebrafish (*Danio rerio*, wild-type) used in this study were bred in our laboratory and were approximately 7-8 months old. The zebrafish breeding conditions, development stage, morphology and hatching rate were examined according to previous research[5]. A 60 L glass water tank contained the aquatic environment, which was filtered by a carbon filter. The water temperature was maintained at 28±1°C with a light/dark cycle 14/10 h. Adult fish were fed blood worms, dry flake food and brine shrimp. Eggs were laid and fertilized within 1 h of the beginning of the light cycle, which provided large populations of synchronously developing embryos. The embryos were collected, pooled and rinsed several times. Embryonic staging was carried out according to the standardized staging series set forth by Kimmel *et al.*[24]. The embryos were immersed in exposure or vehicle control solutions at the 64- to 256-cell stages, and 2.5 hours post-fertilization (hpf). Dead embryos were removed to avoid contaminating the test solutions. Embryos were observed with a microscope (Olympus, SZ61, Japan) to determine the morphological effects.

Chemical Exposure during Development Stage

The NM-silver stock solution for coating and silver ions by electrolysis were diluted with city water, which was allowed to stand for 24 hours to evaporate the chlorine. The final NM-silver exposure concentrations were 10 and 20 ppt. Each group of 300 variable embryos was placed in 1 L glass beakers and maintained in a carbon-filtrated water system at 28±1°C. Embryos were randomly divided into the following groups: Group 1 was the general control group; Groups 2 and 3 were exposed to two concentrations of NM-silver (10 and 20 ppt, respectively); Groups 4 and 5 were

exposed to silver ions produced by electrolysis (10 and 20 ppt, respectively).

Embryos were observed at 2, 5, 8, 22, 27, 32, 48, 52 and 72 hpf, which are time points based on known developmental stages[23]. Dead embryos were removed during development. The hatching rates were calculated at 72 hpf for the experimental and control groups.

Microarray Analysis

For control and test RNAs, the synthesis of target cRNA probes for hybridization were performed using Agilent's Low RNA Input Linear Amplification kit PLUS (Agilent Technology, USA) according to the manufacturer's instructions. Briefly, each 1 μg total RNA and T7 promoter primer mix were incubated at 65°C for 10 min. The cDNA master mix (5X First strand buffer, 0.1 M DTT, 10 mM dNTP mix, RNase-Out, and MMLV-RT) was prepared and added to the reaction mixer. The samples were incubated at 40°C for 2 hours and then the RT and dsDNA syntheses were terminated by incubating at 65°C for 15 min. The transcription master mix was prepared according to the manufacturer's protocol (4X Transcription buffer, 0.1 M DTT, NTP mix, 50% PEG, RNase-Out, Inorganic pyrophosphatase, T7-RNA polymerase, and Cyanine 3-CTP). Transcription of dsDNA was performed by adding the transcription master mix to the dsDNA reaction samples and incubating at 40°C for 2 hours. Amplified and labeled cRNA was purified with the cRNA Cleanup Module (Agilent Technology) according to the manufacturer's protocol. Labeled cRNA target was quantified using a ND-1000 spectrophotometer (NanoDrop Technologies, Inc., Wilmington, DE). After checking the labeling efficiency, fragmentation of cRNA was performed by adding 10X blocking agent and 25X fragmentation buffer and incubating at 60°C for 30 min. The fragmented cRNA was resuspended with 2X hybridization buffer and directly pipetted onto an assembled Agilent's Zebrafish Oligo Microarray Kit V2 (44 K). The arrays were hybridized at 65°C for 17 hours using an Agilent Hybridization oven (Agilent Technology, USA). The hybridized microarrays were washed according to the manufacturer's washing protocol (Agilent Technology, USA).

Data Acquisition and Analysis

The hybridized images were scanned using an Agilent Microarray Scanner (Agilent #G2565BA) and quantified with Feature Extraction Software (Agilent Technology, Palo Alto, CA). All data normalization and selection of fold-changed genes were performed using GeneSpringGX 7.3 (Agilent Technology, USA). Intensity-dependent normalization (LOWESS) was performed, where the ratio was reduced to the residual of the Lowess fit of the intensity vs. ratio curve. The averages of normalized ratios were calculated by dividing the average of normalized signal channel intensity by the average of normalized control channel intensity. Functional annotation of genes was performed according to Gene Ontology™ Consortium (http://www.geneontology.org/index.shtml) by GeneSpringGX 7.3. Gene classification was based on searches done by BioCarta (http://www.biocarta.com/), GenMAPP (http://www.genmapp.org/), DAVID (http://david.abcc.ncifcrf.gov/) and Medline databases (http://www.ncbi.nlm.nih.gov/).

References

1. Lee, H. J., Yeo, S. Y. & Jeong, S. H. Antibacterial effect of nanosized silver colloidal solution on textile fabrics. *J Mater Sci* **38**:2199-2204 (2003).
2. Harper, T. Nano Korea. http://www.nanotechweb. org (2003).
3. Hamouda, T. *et al.* A novel surfactant nanoemulsion with broad-spectrum sporicidal activity against Bacillus species. *J Infect D* **180**:2096-2126 (1999).
4. Sondi, I. & Salopek-Sondi, B. Silver nanoparticles as antimicrobial agent: a case study on E. coli as a model for Gram-negative bacteria. *J Colloid Interf Sci* **275**: 177-182 (2004).
5. Yeo, M. K & Kang, K. Effects of nanometer sized silver materials on biological toxicity during zebrafish embryogenesis. *Bull Korean Chem Soc* **29**:1179-1184 (2008).
6. Rederstorff, M., Krol, A. & Lescure, A. Understanding the importance of selenium and selenoproteins in muscle function. *Cell Mol Life Sci* **63**:52-59 (2006).
7. Radi, A. A. R. & Matkovics, B. Effects of metal ions on the antioxidant enzyme activities, protein contents and lipid peroxidation of carp tissues. *Comp Biochem Physiol C* **90**:69-72 (1988).
8. Roche, H. & Boge, G. Effects of Cu, Zn and Cr salts on antioxidant enzyme activities in vitro of red blood cells of a marine fish. *Dicentrarchus labrax. Toxicol In Vitro* **7**:623-629 (1993).
9. Berger, T. J., Spadaro J. A., Chapin S. E. & Becker R. O. Electrically generated silver ions: quantitative effects on bacterial and mammalian cells. *Antimicrob Agents Ch* **9**: 357-358 (1976).
10. Möller, W., Hofer, T., Ziesenis, A., Karg, E. & Heyder, J. Ultrafine particles cause cytoskeletal dysfunctions in macrophages. *Toxicol Appl Pharm* **182**:197-207 (2002).
11. Lambert, A. L., Mangum, J. B., Delorme, M. P. & Everitt, J. I. Ultrafine carbon black particles enhance respiratory syncytial virus-induced airway reactivity, pulmonary inflammation, and chemokine expression. *Soc Toxicol* **72**:339-346 (2003).

12. Renwick, L. C., Donaldson, K. & Clouter, A. Impairment of alveolar macrophage phagocytosis by ultrafine partic. *Toxicol Appl Pharm* **172**:119-127 (2001).
13. Yeo, M. K. & Park, S. W. Exposing zebrafish to silver nanoparticles during caudal fin regeneration disrupts caudal fin growth and p53 signaling. *Mol Cell Toxicol* **4**: 311-317(2008).
14. Brooker, R. J. & Slayman, C. W. Effects of Mg^{2+} ions on the plasma membrane $[H^+]$-ATPase of Neurospora crassa. II. Kinetic studies. *J Biol Chem* **258**:8833-8838 (1983).
15. Black, C. B., Huang, H. W. & Cowan, J. A. Biological coordination chemistry of magnesium, sodium, and potassium ions. Protein and nucleotide binding sites. *Coord Chem Rev* **135**:165-202 (1994).
16. Hossain, Z. & Huq, F. Studies on the interaction between Ag^+ and DNA. *J Inorg Biochem* **91**:398-404 (2002).
17. Lee, H. C. *et al.* Glycogen synthase kinase 3α and 3β have distinct functions during cardiogenesis of zebrafish embryo. *BMC Dev Biol* **7**:1-15 (2007).
18. Woodgett, J. R. cDNA cloning and properties of glycogen synthase kinase-3. *Methods Enzymol* **200**:564-577 (1991).
19. Woodgett, J. R. Judging a protein by more than its name: GSK-3. *Sci Signal* **12**:1-11(2001).
20. Ramsdell, A. F. Left-right asymmetry and congenital cardiac defects: getting to the heart of the matter in vertebrate left right axis determination. *Dev Biol* **288**: 1-20 (2005).
21. Jia, S., Ren, Z., Li, X., Zheng, Y. & Meng, A. Smad2 and Smad3 are required for mesendoderm induction by transforming growth factor-/nodal signals in Zebrafish. *J Biol Chem* **283**:2418-2426 (2008).
22. Nagaso, H., Suzuki, A., Tada, M. & Ueno, N. Dual specificity of activin type II receptor ActRIIb in dorsoventral patterning during zebrafish embryogenesis. *Develop Growth Differ* **41**:119-133 (1999).
23. Jung, W. K. *et al.* Antifungal activity of the silver ion against contaminated fabric. *Mycoses* **50**:265-269 (2007).
24. Kimmel, W., Ballard, S., Ullman, B. K. & Schilling, T. Stages of embryonic development of the zebrafish. *Dev Dynam* **203**: 253-310 (1995).